Convective transport of very-short-lived bromocarbons to the stratosphere

Qing Liang[1,2], Elliot Atlas[3], Donald Blake[4], Marcel Dorf [5,6], Klaus Pfeilsticker [5], Sue Schauffler[7]

[1] {NASA Goddard Space Flight Center, Atmospheric Chemistry and Dynamics, Greenbelt, MD, USA}
[2] {Universities Space Research Association, GESTAR, Columbia, MD, USA}
[3] {University of Miami, 4600 Rickenbacker Causeway, Miami, FL 33149, USA}
[4] {University of California, 570 Rowland Hall, Irvine, CA 92697, USA}
[5] {Institut für Umweltphysik, University of Heidelberg, Heidelberg, Germany}
[6] {Now at Max-Planck-Institut für Chemie, Mainz, Germany}
[7] {Earth Observing Laboratory, NCAR, Boulder, CO, USA}

Correspondence to: Q. Liang (Qing.Liang@nasa.gov)

Abstract. We use the NASA GEOS Chemistry Climate Model (GEOSCCM) to quantify the contribution of two most important brominated very short-lived substances (VSLS), bromoform ($CHBr_3$) and dibromomethane (CH_2Br_2), to stratospheric bromine and its sensitivity to convection strength. Model simulations suggest that the most active transport of VSLS from the marine boundary layer through the tropopause occurs over the tropical Indian Ocean, the tropical western Pacific, and off the Pacific coast of Mexico. Together, convective lofting of $CHBr_3$ and CH_2Br_2 and their degradation products supplies ~8 ppt total bromine to the base of the Tropical Tropopause Layer (TTL, ~150 hPa), similar to the amount of VSLS organic bromine available in the marine boundary layer (~7.8-8.4 ppt) in the above active convective lofting regions. Of the total ~8 ppt VSLS bromine that enters the base of TTL at ~150 hPa, half is in the form of organic source gases and half as inorganic product gases. Only a small portion (<10%) of the VSLS-originated bromine is removed via wet scavenging in the TTL before reaching the lower stratosphere. On global and annual average, $CHBr_3$ and CH_2Br_2, together, contribute ~7.7 pptv to the present-day inorganic bromine in the stratosphere. However, varying model deep convection strength between maximum (strongest) and minimum (weakest) convection conditions can introduce a ~2.6 pptv uncertainty in the contribution of VSLS to inorganic bromine in the stratosphere (Br_y^{VSLS}). Contrary to the conventional wisdom, minimum convection condition leads to a larger Br_y^{VSLS} as the reduced scavenging in soluble product gases, thus a significant increase in product gas injection (2-3 ppt), greatly exceeds the relative minor decrease in source gas injection (a few 10ths ppt).

1. Introduction

Very short-lived (VSL) bromocarbons originate mostly from ocean biogenic sources, and when transported into the stratosphere, they exert a significant impact on the bromine budget and stratospheric ozone depletion (Kurylo and Rodriguez, 1999; Sturges et al., 2000). Recent years have seen significant progress in modeling efforts to quantify the contribution of brominated VSL substances (VSLS) to stratospheric inorganic bromine (Br_y^{VSLS}) (e.g. Warwick et al., 2006; Liang et al., 2010; Aschmann et al., 2011; Aschmann and Sinnhuber, 2013; Hossaini et al., 2012a, 2012b, 2013). These modeling studies suggest that brominated VSLS contribute 4.8-7 ppt to reactive stratospheric bromine, within the 1-8 ppt estimate range from satellite and balloon-borne observations (WMO 2011; Sinnhuber et al., 2005; Sioris et al., 2006; Dorf et al., 2006a, 2008; Salawitch et al., 2010).

The most important VSLS pathway to the stratosphere is via convective lofting through the tropical tropopause layer (TTL). Atmospheric chemistry and transport of brominated VSLS involves the coupling of various complex processes, e.g. highly un-uniform ocean emissions, convective transport of source gases and product gases, as well as wet scavenging of soluble product gases. An accurate modeling representation of these processes remains a challenging task. Modeling of these processes in general requires some extent of simplified assumptions and/or parameterizations, which may differ greatly from one model study to another. These differences have lead to significant differences in the modeled Br_y^{VSLS} estimates. For example, a recent model study by Hossaini et al. (2013) found that modeled Br_y^{VSLS} could vary by a factor of 2 when using four recently published emission inventories (Liang et al., 2010; Pyle et al., 2011; Ordóñez et al., 2012; Ziska et al., 2013). In general, model studies agree relatively well on source gas injection (SGI), suggesting about ~50% of bromoform ($CHBr_3$) and ~90% of dibromomethane (CH_2Br_2) can reach the stratosphere through SGI (e.g. Dvortsov et al., 1999; Nielsen and Douglass, 2001; Aschmann et al., 2011; Hossaini et al., 2010, 2012a). However,

modeled contribution on product gas injection (PGI) is highly uncertain depending on how wet scavenging is implemented. Many early model studies assume a uniform washout lifetime against wet scavenging (e.g. Dvortsov et al., 1999; Nielsen and Douglass, 2001; Hossaini et al., 2010; Aschmann et al., 2009), which was inadequate and lead to an underestimate in modeled Br_y^{VSLS} (Hossaini et al., 2012a; Aschmann et al., 2011). A recent study by Aschmann and Sinnhuber (2013) shows that treating Br_y^{VSLS} as a single soluble tracer (e.g. Liang et al., 2010) can also lead to an underestimate. They found that Br_y^{VSLS} increased from 3.4 ppt to 5 ppt when switching from an idealized setup with a single soluble inorganic bromine tracer to a full chemistry scheme. Thus, an accurate modeling of transport and wet scavenging of PGI seems to be the key in narrowing the uncertainty of model estimate of Br_y^{VSLS}.

Understanding how the contribution of VSLS to stratospheric bromine varies with convection strength has significant climate implications. A recent modeling analysis by Hossaini et al (2012b) suggests that VSLS SGI increases from ~1.7 ppt in 2000 to ~2.0-2.7 ppt in 2100 using the Intergovernmental Panel on Climate Change (IPCC) representative concentration pathways (RCPs) scenarios, as the future simulations feature stronger tropical deep convection transport to the lower stratosphere. On the other hand, the overall response of Br_y^{VSLS} to convection strength is somewhat murky. Earlier studies deploying a uniform washout lifetime found different washout rates result a significant range in the contribution of $CHBr_3$ to Br_y, 0.5-3 ppt in Sinnhuber and Folkins (2006) and 1.6-3 ppt in Aschmann et al., (2011). Liang et al. (2010) which deploys explicit wet scavenging in convective updrafts found that convective scavenging only accounts for ~0.2 ppt difference in modeled Br_y^{VSLS}. Similar results were reported in Aschmann et al. (2011), who showed while SGI is highly correlated with convective activity, the impact on total stratospheric bromine in a full chemistry scheme is nearly insensitive to dehydration, likely due to convection dilution and increased scavenging.

In this study, we use a 3-dimensional Chemistry Climate Model with fully interactive $CHBr_3$ and CH_2Br_2, the two most important brominated VSLS, to better understand how VSLS and their degradation products enter the stratosphere. We will also test the uncertainty in modeled Br_y^{VSLS} due to varying strength in convection and scavenging.

2. Model and Simulations

2.1 Model Description

We conduct model simulations using the NASA GEOS Chemistry Climate Model (GEOSCCM) Version 2, which couples the GEOS-5 GCM (Reinecker et al., 2008) with a stratospheric chemistry module. Model simulations have a horizontal resolution of 2.5°×2° (longitude by latitude) with 72 vertical layers from surface to 0.01 hPa. The GEOS-5 model uses a flux-form semi-Lagrangian dynamical core (Lin, 2004) and the Relaxed Arakawa Schubert (RAS) parameterization for convection (Moorthi and Suarez, 1992). The GEOS-5 moist processes are represented using a convective parameterization and prognostic cloud scheme.

The GEOSCCM V2 stratospheric chemistry module includes all important gas phase stratospheric reactions as described in Douglass and Kawa (1999), and chemical calculations are carried out above the 27th eta layer (approximately 350 hPa on global average). All chemical kinetics and photolysis rates are calculated following JPL 2010 (Sander et al., 2011). We modify the standard V2 chemistry scheme to include $CHBr_3$ and CH_2Br_2, both are interactive with the full stratospheric chemistry scheme. The two organic source gases are released at the ocean surface following the geographically resolved emission distribution described in Liang et al. (2010) and are destroyed in the atmosphere via photolysis and reaction with the hydroxyl radical

(OH). OH above ~350 hPa is calculated online in the stratospheric chemistry module. OH in the lowest 26 layers (troposphere) is relaxed to a monthly mean climatological fields documented in Spivakovsky et al. (2000). Global annual mean OH from Spivakovsky et al. (2000) is 1.16×10^6 molecules cm^{-3}, yielding an atmospheric methyl chloroform (CH_3CCl_3) lifetime of ~5.5 years. In most of the troposphere, only simple bromine chemistry is considered which partitions 80% of inorganic bromine products into HBr and the remaining 20% as HOBr, ratios adopted from Yang et al. (2005). Above the 27th eta layer (~350 hPa), bromine from $CHBr_3$ and CH_2Br_2 degradation is released as Br and interacts fully with stratospheric chemistry. Compare to the idealized case in Liang et al. (2010) that tracks the atmospheric transport of Br_y^{VSLS} in a single highly soluble tracer, in this experiment, we deploy a detailed speciation of Br_y^{VSLS} in both soluble forms (HBr, HOBr, and $BrONO_2$) and insoluble forms (Br, BrO, BrCl) in the fully interactive stratospheric chemistry scheme in the TTL and stratosphere. Although $BrONO_2$ is not produced in the troposphere in the current simple chemistry scheme, $BrONO_2$ produced in the stratosphere is allowed to transport to lower altitudes via large-scale descent. A previous detailed tropospheric chemistry model study using the Harvard GEOS-Chem model and VSLS emissions from Liang et al (2010) shows a small fraction of Br_y exists as BrO (0.1-0.2 ppt) below 10 km in the tropics (Parrella et al., 2012). However, the impact of the absence of this tropospheric BrO on stratospheric bromine is likely small. No heterogeneous chemistry for VSLS is included in our simulations, but results from Aschmann and Sinnhuber (2013) suggest that the impact of heterogeneous chemistry is minor and the inclusion of heterogeneous activation prevents loss in scavenging and can increase Br_y^{VSLS} by 10%. While heterogeneous chemistry can shift Br_y partition and increase HBr up to 4 times between 12-18 km in the tropics (Aschmann et al, 2011), the absence of heterogeneous chemistry in GEOSCCM is likely to have only a small impact on Br_y^{VSLS} since the model HBr is present at very low abundance during daytime when the majority of convective scavenging take place (see section 3.1 and Figure 4) and the overall convective scavenging in the TTL is rather inefficient (see section 3.2).

The wet scavenging of the soluble inorganic bromine are the same as that detailed in Liang et al. (2010). It includes scavenging in rainout (in-cloud precipitation) and washout (below-cloud precipitation) in both large-scale precipitation (Giorgi and Chameides, 1986) and deep convective updrafts (Balkanski et al., 1993). We assume high solubility for all three inorganic bromine reservoir species, HBr, HOBr, and $BrONO_2$. At each time step, we follow the Giorgi and Chameides (1986) parameterization to compute the wet scavenging using the GEOS-5 model calculated large-scale and convective precipitation rates and the parameterized fraction of grid square area, *F*, that actually experience precipitation (Balkanski et al., 1993). Previous studies using the Giorgi and Chameides (1986) parameterization showed that, for large-scale precipitation, the global mean *F* is about 2.5% for all grid boxes and the median value is 10%, with values exceeding 40% in ~10% of the grid boxes (Balkanski et al., 1993; Liu et al., 2001). The global mean *F* for convective precipitation is much smaller, only 0.4% (Liu et al., 2001). When evaporation occurs during large-scale and convective transport, the corresponding fraction of the dissolved inorganic bromine is released back to the atmosphere. This wet scavenging scheme has been applied in many atmospheric modeling studies of soluble trace gases and aerosols, e.g. ^{210}Pb, ^{7}Be, sulfate, sea salt, dust, and the simulated concentrations compare well with surface observations at many observation sites around the globe (e.g. Balkanski et al., 1993; Chin et al., 2000; Ginoux et al., 2001; Liu et al., 2001).

In this study, we present results from two 51-year simulations between 1960-2010, one with brominated VSLS chemistry (R_{VSLS}) and one without (R_{BASE}), to examine troposphere to

stratosphere transport (TST) of VSLS and their contribution to stratospheric bromine. It takes a considerable long time (~15 years) for the full impact of VSLS to reach the upper stratosphere, thus the first 16 years are considered as spin-up. A full model evaluation and discussion of the impact of VSLS on stratospheric ozone are presented in a separate paper, currently in preparation. For this study, we focus on model results from the last 10 years of the two simulations.

2.2 Convection Sensitivity Simulations

To quantify the uncertainty in Br_y^{VSLS} due to changes in convection strength, we conduct two sensitivity simulations from 1980 to 2010 to represent minimum convection (R_{MINCNV}) and maximum convection (R_{MAXCNV}) conditions by varying five convective parameters in RAS that impact the strength of deep convection, clouds, convective condensate and re-evaporation (Ott et al., 2009; 2011). These five convective parameters are RASAL1 and RASAL2 (regulates the strength and vertical profile of the relaxation time scale for deep convection), ACRITFAC (used to compute the critical value of the cloud work function which determines the initiation of convection), BASE_EVAP_FAC (regulates the amount of rain evaporated into the environment below the cloud base), and AUTOC_CN (used to calculate the autoconversion of convective condensate). These five are identified as the most strongly influencing out of the total 16 parameters examined using a large number of "Monte Carlo" type simulations and ensemble simulations in both a Single-Column Model as well as the GEOS-5 GCM (Ott et al., 2011). In the two sensitivity simulations, the five parameters are varied to produce the strongest (MAXCNV) and the weakest (MINCNV) representations of convection considered reasonable. In general, compared to the minimum convection condition, the maximum convection condition yields significantly large increases in shallow convection below 5 km and ~20-30% stronger vertical mass flux and more horizontal divergence between 12.5-16.5 km (Ott et al., 2011). The values used for the five convective parameters for the minimum and maximum conditions have been tested extensively in the previous ensemble analysis that they produce reasonable precipitation patterns when compared with data from the Global Precipitation Climatology Project (GPCP) that were compiled from satellite and rain gauge observations (Ott et al., 2011). The correlation coefficients between the standard run, MAXCNV and MINCNV simulations and the GPCP data sets are 0.65, 0.64, 0.62, respectively (Ott et al., 2011).

We aim to use these minimum and maximum conditions to bound the range of uncertainty that can be introduced due to variations in the strength of convection and wet scavenging.

3. Results

3.1 The Contribution of VSLS to Stratospheric Bromine

The simulated $CHBr_3$ and CH_2Br_2 have been evaluated extensively in Liang et al. (2010) and compares well with aircraft and surface observations in their atmospheric distribution, geographically and vertically, as well as the associated seasonality. Here we present a summary comparison of observed and modeled $CHBr_3$ in the troposphere for 30-60ºS, 30ºS-30ºN, 30-60ºN, and 60-90ºN latitude bands (Figure 1). The observed profiles are compiled using Whole Air Sampler canister measurements (Schauffler et al., 1999; Blake et al., 2003) from eight NASA aircraft missions, as detailed in Liang et al. (2010), and averaged within each latitude band at 1-km vertical interval. The comparison clearly shows that the model captures well the source gas concentrations and vertical gradients in the tropics, mid and high latitudes in both hemispheres.

Figure 2 shows a comparison of our simulated BrO with balloon measurements from the LPMA (Limb Profile Monitor of the Atmosphere) / DOAS (Differential Optical Absorption

Spectroscopy) at Teresina (5.1°S), Aire sur l'Adour (43.7°N), and Kiruna (67.9°N) collected between 2003-2005 (Dorf et al., 2006a, 2006b, 2008; Rozanov et al., 2011). The lower levels of BrO from R_{BASE} in comparison to the measurements indicate the essential role of VSLS in completing the stratospheric bromine budget. With VSLS, the GEOSCCM model simulates well the observed BrO at all sampled locations in the tropics, mid and high latitudes. Currently the GEOSCCM does not include the remaining 3 of the 5 major brominated VSLS, CH_2BrCl, $CHBr_2Cl$ and $CHBrCl_2$ (lifetimes between 70-150 days). Assuming a total tropospheric abundance of 1 ppt of these three VSLS and ~90% (value for CH_2Br_2) of the source gases survive the TST to the stratosphere, this adds ~0.9 ppt to the current model estimate of stratospheric Br_y of ~24 ppt. With the current model BrO/Br_y ratio, such an increase will lead to an increase in BrO in the stratosphere up to 0.6 ppt (not shown). This results a better agreement with the DOAS BrO measurements in Teresina and Aire sur l'Adour and reasonable agreement at Kiruna, considering the large spatial variability in BrO in the high latitudes and rather localized balloon measurements. Since the model is running freely by specifying only surface source gas emissions, the fact that the model simulates well the observed concentrations for both the source gases and BrO suggests that the model presents a credible representation of stratospheric bromine chemistry.

Comparing results from the R_{VSLS} and R_{BASE} runs (Figure 3), we find that the inclusion of $CHBr_3$ and CH_2Br_2 adds a uniform ~7.7 ppt Br_y throughout most of the stratosphere. The current Br_y^{VSLS} estimate is 55% higher than our previous estimate of ~5 ppt (Liang et al., 2010) and ~6 ppt estimate in Hossaini et al. (2013), though the latter two are driven by the same VSLS emissions. Compared to the idealized case in Liang et al. (2010) that tracks Br_y^{VSLS} in a single highly soluble tracer, Br_y^{VSLS} in this study is present in the fully interactive stratospheric chemistry scheme in both soluble forms (HBr, HOBr, and $BrONO_2$) and insoluble forms (Br, BrO, BrCl) in the TTL. The ratio of insoluble and soluble Br_y varies with time of the day as well as altitude and location. Figure 4 shows the contrast of model inorganic bromine speciation in the tropics between daytime and nighttime. In the TTL region, at daytime, when most convective lofting occurs, the majority of Br_y exists as insoluble Br and BrO (Figure 4a), therefore greatly increases the amount of Br_y^{VSLS} that survives wet scavenging during the TST and ultimately reaches the stratosphere. The increase from ~5 ppt to ~7.7 ppt when switching from an idealized case to fully interactive stratospheric chemistry is consistent with results from Aschmann and Sinnhuber (2013), who found that Br_y^{VSLS} increased from 3.4 ppt to 5 ppt when switching from an idealized setup with a single soluble inorganic bromine tracer to a full chemistry scheme. The different estimates between Hossaini et al. (2013) and this work are likely due to how the ratio of soluble and insoluble inorganic bromine is determined inside the two models. Compared to this work which partitions inorganic bromine in its various forms based on chemical reaction rates, Hossaini et al. (2013) used a mean altitude-dependent HBr:Br_y ratio. This likely leads to an excessive washout of Br_y^{VSLS} as during daytime when most of the convective lofting occurs, the majority of the inorganic bromine exists as insoluble Br and BrO. This suggests that a close approximate of soluble and insoluble inorganic product gases and the associated diurnal variation are critical to accurately quantify the contribution of VSLS to stratospheric halogen in VSLS modeling.

A recent study by Kreycy et al. (2013), using balloon borne DOAS BrO measurements over Kiruna (67.9ºN, 22.1ºE), suggests that the ratio of $J(BrONO_2)/k_{BrO+NO2}$ should be a factor of 1.7 larger than the JPL 2010 recommendations and is likely to shift more $BrONO_2$ into BrO. However, this result will have only a small impact on our Br_y^{VSLS} estimates. Currently, $BrONO_2$

only accounts for ~0.5 ppt of the total Br_y^{VSLS} in the TTL during daytime. In addition, convective scavenging of the inorganic bromine in the TTL is not an efficient removal process (section 3.2). Increasing the ratio of $J(BrONO_2)/k_{BrO+NO2}$ in the model will shift Br_y^{VSLS} partition from $BrONO_2$ to BrO, which in turn will result an increase in Br_y^{VSLS} due to less $BrONO_2$ scavenging. However, this increase will be small (at most a few tenths ppt).

3.2 Troposphere-to-Stratosphere Transport of VSLS

We use the simulated monthly mean $CHBr_3$ distribution on the 355 K potential temperature surface (just below TTL) to show important tropical regions where active TST initiates (Figure 5). Theoretically, trace gas distribution on the 365 K surface should be more indicative of TST as 365 K marks the zero radiative heating and air mass elevated above this level can enter the lower stratosphere through slow radiative ascent (e.g. Gettelman and Forster, 2002; Fueglistaler et al., 2009). However, it is difficult to identify active TST regions on the 365 K map (not shown) as a significant portion of $CHBr_3$ is converted to product gases. This is not surprising for a short-lived compound with lifetime ~ 26 days (WMO 2011) while on average it takes about 10 days for air to transport by ±10 K (Fueglistaler et al., 2004; Levine et al., 2007). Compared to $CHBr_3$, it is much more difficult to identify active TST regions on a CH_2Br_2 map, as CH_2Br_2 distribution appears more zonal with a smaller meridional gradient due to a longer lifetime, ~ 120 days (WMO 2011) and up to ~ 450 days locally in the TTL (Hossaini et al., 2010), and thus more mixing with the surrounding background air (not shown). The 355K $CHBr_3$ map shows three active regions that can efficiently deliver VSLS to the base of TTL: 1) the tropical Indian Ocean, 2) the tropical western Pacific, and 3) off the Pacific coast of Mexico (Figure 5). There is significant seasonality associated with each entry region. The Indian Ocean appears as the most active region for the TST of $CHBr_3$ and occurs all year long with a maximum in boreal winter (DJF). Lofting in the tropical western Pacific reaches its maximum in boreal summer (JJA), while the TST off the Mexico coast occurs mostly in boreal summer (JJA) and fall (SON). The importance of convective lofting in the Western Pacific warm pool in TST has been noted in many previous studies (e.g. Hatsushika and Yamazaki, 2003; Fueglistaler et al., 2004; Aschmann et al., 2009; Hossaini et al., 2012a; Ashfold et al., 2012) with several others suggesting that the Indian Ocean is also an important region in the TST of VSLS (Levine et al., 2007, 2008; Brioude et al., 2010; Hoyle et al., 2011).

We show in Figure 6 the vertical profiles of organic source gases (CH_2Br_2×2, $CHBr_3$×3) and inorganic product gases in the three critical convective lofting regions to illustrate the transport and wet scavenging of the brominated VSLS during the TST and the relative importance of SGI vs. PGI. Although tropospheric Br_y are assumed highly soluble, only a fraction of the grid boxes and a fractional area of the precipitating grid boxes actually experiencing precipitation and scavenging. On average, of all inorganic bromine (~4 ppt) produced from $CHBr_3$ and CH_2Br_2 in the tropical troposphere, about 50% (~2 ppt) is removed below 500 hPa, mainly by large-scale precipitation (Liang et al., 2010), with an additional few tenths ppt scavenged in the upper troposphere. Together, ~1.5 ppt of HBr and HOBr survive large-scale and convective scavenging and remain in the tropical upper troposphere. Br, BrO, and $BrONO_2$ produced from $CHBr_3$ and CH_2Br_2 degradation in the tropical upper troposphere adds an additional ~2 ppt to Br_y^{VSLS}. Over the tropical Indian Ocean, on annual average, the mixing ratio of total bromine from VSLS (organic + inorganic) at 150 hPa (~355K) is ~8.5 ppt, the same as its surface abundance (~8.5 ppt). This implies convective lofting in this region is so efficient that the amount of VSL bromine that enters the base of TTL is set by the concentration at the marine boundary layer. As air ascend to higher altitudes, a small portion of Br_y^{VSLS} (~0.8 ppt, 10%) is

gradually removed from the atmosphere via wet scavenging until reaching a constant 7.7 ppt above 10 hPa. The somewhat wavy structure in the total bromine profile in the lower stratosphere implies that not all wet scavenging happens locally and the dip in total bromine concentration between 100-50 hPa is likely associated with recirculation of air back from the mid-latitude lower stratosphere where additional scavenging occurs via in-cloud rainout. Results from the tropical western Pacific and off the coast of Mexico are similar, with a smaller surface abundance of organic bromine (7.8~8.1 ppt) and slightly less washout around 100 hPa. The global averaged total bromine from VSLS (Br^{VSLS}) profile shows a maximum value of ~8 ppt at ~100 hPa. To supply this amount of Br^{VSLS} to the lower stratosphere, transport from the marine boundary layer has to initiate from tropical regions where active convective lofting is co-located with high surface concentrations, where the collective $CHBr_3$ and CH_2Br_2 abundance exceeds 8 ppt Br.

Mapping streamlines on top of the VSLS organic bromine distribution in the tropics clearly illustrates the importance of co-location of deep convection with high surface concentration regions (Figure 7). Among the three ascending branches of the Walker circulation (Webster 1983), while ascent in the tropical western Pacific penetrates deepest into the TTL, ascent in the Indian Ocean is capable in delivering more VSLS bromine to the base of TTL due to higher surface concentrations. The surface abundance of VSLS bromine is largely dependent on the emission distribution used. Liang et al. (2010) assumed uniform zonal emission strength across all longitudes, but the rate of bromocarbon emissions for the coastal regions per unit area are much higher than that in the open oceans. In the tropics, the prevailing surface easterly trade winds tend to bring recent emissions of $CHBr_3$ from the adjacent Indonesian coastal regions while the tropical western Pacific Ocean sees recent emissions of $CHBr_3$ from the open ocean. Therefore, the surface concentrations are higher in the Indian Ocean than the tropical western Pacific. However, it is important to point out that only a few surface observation constraints from the tropical western Pacific and none from the tropical Indian Ocean were available to derive the Liang et al., (2010) emission scenario. Hossaini et al. (2013) conducted a recent model study comparing four independent brominated VSLS emission estimates. Of all four emission inventories examined (Liang et al., 2010; Pyle et al., 2011; Ordóñez et al., 2012; Ziska et al., 2013), modeled $CHBr_3$ and CH_2Br_2 concentrations using the emission estimates from Liang et al. (2010) compare very well against tropical observations from multiple years of National Oceanic and Atmospheric Administration/Earth System Research Laboratory (NOAA/ESRL) surface flask measurements. The global mean model biases (model – observations) are –0.25 ppt for $CHBr_3$ (ranging from +0.12 ppt in the tropics to –0.65 ppt in the northern high latitudes) and –0.02 ppt for CH_2Br_2 (ranging from +0.14 ppt in the tropics to -0.11 ppt in the northern and southern high latitudes). Comparison with the HIAPER Pole-to-Pole Observations (HIPPO) measurements between 2009–2011 supported by the National Science Foundation (NSF) yields even better agreement, with little biases in global mean $CHBr_3$ ($\Delta_{model\text{-}obs}$ = +0.04 ppt) and CH_2Br_2 ($\Delta_{model\text{-}obs}$ = –0.01 ppt). The modeled biases for each latitude band are also small, –0.16 - +0.30 ppt for $CHBr_3$ and –0.10 - +0.12 ppt for CH_2Br_2. When compared against the aircraft measurements collected in the tropical western Pacific during the Stratospheric Ozone: Halogen Impacts in a Varying Atmosphere (SHIVA) campaign, Liang et al. (2010) yields the best CH_2Br_2 (mean bias of +0.2 ppt compared with observations), compared to the other three emissions, but the simulated $CHBr_3$ is ~ +0.76 ppt too high on average. Note the high bias in modeled $CHBr_3$ in the tropical western Pacific will likely lead to a high bias in the model Br_y^{VSLS}, although the lofting in Indian Ocean seems to be more critical in determining the total amount of VSLS

bromine in the lower stratosphere in this study. The model simulated high concentration of brominated VSLS over the Indian Ocean is yet to be evaluated when more surface observations become available and the importance of the Indian Ocean in delivering higher amounts of VSLS bromine into the TTL needs to be assessed. The simulated high surface concentrations of $CHBr_3$ and CH_2Br_2 near tropical Central America were validated with the NASA TC[4] and INTEX-B measurements (Liang et al., 2010). This region, compared to the above two, is much less efficient in delivering VSLS bromine into the TTL due to the relatively weaker ascent. However, this ascending branch can be important in particular seasons and in individual years as the Walker circulation moves in the east-west direction between different phases of the El Niño Southern Oscillation (ENSO). For example, using trajectory calculations, Levine et al. (2008) found a clear shift in the TTL origin of air parcels from the tropical western Pacific and Indonesia to those from the Eastern Pacific and South America in El Niño years.

Of the total VSLS bromine that enters the base of TTL, about half (~4 ppt) is in the form of inorganic product gases (Figure 6) despite our simple assumption that all inorganic bromine reservoir species are highly soluble and all inorganic bromine produced below 350 hPa are partitioned into the soluble forms - HBr and HOBr. A commonly adopted approach in many previous modeling studies is to prescribe the VSLS concentration at the base of TTL with observed organic source gas mixing ratios in the upper troposphere and tracks the subsequent chemistry and transport (e.g. Sinnhuber and Folkins, 2006; Aschmann et al. 2011, Aschmann and Sinnhuber, 2013). Our result implies that Br_y^{VSLS} estimate from such approach is not complete as it misses an important component associated with PGI, which is as large as SGI at the base of TTL in our model simulation. A second implication of this result is that if we were to use measurements from the TTL region to quantify the contribution of VSLS to stratospheric bromine, it is necessary to make measurements of both organic and inorganic forms to fully account for the impact of VSLS on the atmospheric bromine budget.

3.3 The Impact of Convection Strength

We examine the difference between the two convection sensitivity simulations, R_{MINCNV} and R_{MAXRUN}, to illustrate the impact of deep convection on Br_y^{VSLS} (Figure 8). Difference between these two simulations (R_{MINCNV} - R_{MAXRUN}) suggests that in regions that mattered most (the three tropical convection centers), surprisingly, the minimum convection condition is more favorable for the TST of VSLS. While weaker convection slightly decreases SGI (a few tenths ppt), PGI increases significantly (2-3 ppt) due to less scavenging under minimum convection condition. TST of the longer-lived CH_2Br_2 is less sensitive to convection strength compared to that of $CHBr_3$ because of its longer lifetime. The significant increase in $CHBr_3$ and CH_2Br_2 in the mid-latitude bands under minimum convection mainly reflects the compensating responses in large-scale descent in a general circulation model as a result of changing convection strength (Ott et al., 2011). The decrease of the descent does not impact TST of VSLS. Aschmann et al. (2011) found a qualitatively similar behavior for changes of VSLS SGI and PGI under El Niño vs. La Niña conditions - while SGI increased slightly under enhanced deep convection, the sum of SGI and PGI decreased. However, the net decrease in the Br_y^{VSLS} (<0.5 ppt) due to changes in convection strength between El Niño vs. La Niña conditions reported in Aschmann et al. (2011) is much smaller than our results above, most likely due to a much higher Br_y^{VSLS} abundance in the TTL in this work.

Globally, the differences in convection strength and wet scavenging introduce a ~2.6 ppt uncertainty in Br_y^{VSLS} (~6.5 ppt in R_{MAXRUN} and ~9.1 ppt in R_{MINRUN}) (Figure 3). Although these two simulations represent the two extreme parameterization conditions within reasonable range,

BrO from both simulations still falls within the uncertainty range of the DOAS balloon observations of ±2.5 ppt (Figure 2, Dorf et al., 2006b).

4. Conclusions

We use the NASA Goddard 3-D Chemistry Climate Model, GEOSCCM, to quantify the contribution of brominated very short-lived substances (VSLS) to reactive stratospheric bromine and to test its sensitivity to the strength of deep convection and the associated scavenging.

The inclusion of $CHBr_3$ and CH_2Br_2 in a fully interactive stratospheric chemistry module deployed in the TTL and the stratosphere adds ~7.7 pptv to the present-day stratospheric inorganic bromine. The most active transport of VSLS from the marine boundary layer through the tropical tropopause layer (TTL) occurs where high surface concentrations of VSLS co-locate with deep convection centers: 1) the tropical Indian Ocean, 2) the tropical western Pacific warm pool, and 3) off the Pacific coast of Mexico. On annual average, almost all VSLS-originated bromine available in the marine boundary layer (~7.8-8.4 ppt) at these active convective lofting regions enters the TTL, half in the form of source gas injection (SGI) and half in the form of product gas injection (PGI). After lofting above 150 hPa (~355K), the majority of the VSLS-originated bromine survives TST and reaches the lower stratosphere, with only a small portion (~0.8 ppt, 10%) removed by wet scavenging. Our model results point to a clear need for more surface measurements in the active VSLS lofting regions, in particular the tropical Indian Ocean and the tropical western Pacific, for improved emissions estimate as well as a better quantification of how much VSLS bromine is available before ultimately enters the stratosphere through the TTL.

Our current estimate of the contribution of $CHBr_3$ and CH_2Br_2 to stratospheric bromine (Br_y^{VSLS}) is higher than previous modeling estimates, mainly reflecting the differences in how transport and wet scavenging of product gases are treated in different models (Hossaini et al., 2012a; Aschmann and Sinnhuber, 2013). Interestingly, even though the models are driven with same emission estimates (Liang et al., 2010; Hossaini et al, 2013) and/or with similar source gas abundance at the base of TTL (Aschmann et al. 2011; Aschmann and Sinnhuber, 2013), this study still yields higher Br_y^{VSLS} for two main reasons. Modeling VSLS and their degradation products in a full stratospheric chemistry scheme in the TTL and stratosphere leads to a better representation of the partition between soluble and insoluble product gases and the associated diurnal variation, both are critical in an accurate Br_y^{VSLS} estimate. Secondly, tracking PGI from the free troposphere to the base of TTL, which is as large as SGI at the base of TTL in our model simulation, is also important. This was not included in many earlier model studies (e.g. Aschmann et al. 2011; Aschmann and Sinnhuber, 2013), thus implying a missing component in these earlier model VSLS contribution estimates.

Differences in model deep convection strength can introduce ~30% (6.6 ppt - 9.2 ppt) uncertainty in simulated Br_y^{VSLS} within the same convection scheme. It is important to point out that this uncertainty is likely larger among different models or a same model but different versions when different convective parameterizations are used.

Contrary to conventional wisdom that the VSLS impact on stratospheric bromine is larger under more intense deep convection, our simulations suggest that minimum convection condition is favorable for TST of VSLS due to reduced scavenging of soluble product gases under weaker convection. The impact of convection strength on PGI greatly outweighs the impact on SGI with the change in PGI ~ ten times larger than that of SGI.

Acknowledgements. Funding for this research is from the NNX11AN71G project supported by the NASA ACMAP program. Funding for the DOAS team are from the German Ministry of Economy (BMWi) (50EE0840), the European Space Agency (ESA-ESRIN: no. RFQ/3-12092/07/I-OL) and the Deutsche Forschungsgemeinschaft, DFG (grants PF-384/5-1 and 384/5-1 and PF384/9-1/2), as well as Additional funding from the EU projects Reconcile (FP7-ENV-2008-1-226365) and SHIVA (FP7-ENV-2007-1-226224). We thank Bjoern-Martin Sinnhuber and the other anonymous reviewer for their great and constructive comments.

438 **References**

439 Aschmann, J., Sinnhuber, B.-M., Atlas, E. L., and Schauffler, S. M.: Modeling the transport of
440 very short-lived substances into the tropical upper troposphere and lower stratosphere,
441 Atmos. Chem. Phys., 9, 9237–9247, doi:10.5194/acp-9-9237-2009, 2009.
442 Aschmann, J., Sinnhuber, B.-M., Chipperfield, M. P., and Hossaini, R.: Impact of deep
443 convection and dehydration on bromine loading in the upper troposphere and lower
444 stratosphere, Atmos. Chem. Phys., 11, 2671–2687, doi:10.5194/acp-11-2671- 2011, 2011.
445 Aschmann, J., and Sinnhuber, B.-M.: Contribution of very short-lived substances to stratospheric
446 bromine loading: uncertainties and constraints, Atmos. Chem. Phys., 13, 1203-1219,
447 doi:10.5194/acp-13-1203-2013, 2013.
448 Ashfold, M. J., Harris, N. R. P., Atlas, E. L., Manning, A. J., and Pyle, J. A.: Transport of short-
449 lived species into the Tropical Tropopause Layer, Atmos. Chem. Phys., 12, 6309-6322,
450 doi:10.5194/acp-12-6309-2012, 2012.
451 Balkanski, Y. J., Jacob, D. J., Gardner, G. M., Graustein, W. C., and Turekian, K. K.: Transport
452 and residence times of tropospheric aerosols inferred from a global three-dimensional
453 simulation of ^{210}Pb, J. Geophys. Res., 98, 20,573-20,586, doi:10.1029/93JD02456, 1993.
454 Blake, N. J., Blake, D. R., Simpson, I. J., Meinardi, S., Swanson, A. L., Lopez, J. P., Katzenstein,
455 A. S., Barletta, B., Shirai, T., Atlas, E., Sachse, G., Avery, M., Vay., S., Fuelberg, H. E.,
456 Kiley, C. M., Kita, K., Rowland, F. S.: NMHCs and halocarbons in Asian continental
457 outflow during the Transport and Chemical Evolution over the Pacific (TRACE-P) field
458 campaign: comparison with PEM-West B, J. Geophys. Res., 108, 8806,
459 doi:10.1029/2002JD003367, 2003.
460 Brioude, J., Portmann, R. W., Daniel, J. S., Cooper, O. R., Frost, G. J., Rosenlof, K. H., Granier,
461 C., Ravishankara, A. R., Montzka, S. A. and Stohl, A: Variations in ozone depletion
462 potentials of very short-lived substances with season and emission region." Geophysical
463 Research Letters, 37, L19804, doi:10.1029/2010GL044856, 2010.
464 Chin, M., Savoie, D. L., Huebert, B. J., Bandy, A. R., Thornton, D. C., Bates, T. S., Quinn, P. K.,
465 Saltzman, E. S., and De Bruyn, W. J.: Atmospheric sulfur cycle in the global model
466 GOCART: Comparison with field observations and regional budgets, J. Geophys. Res., 105,
467 24 689–24 712, 2000.
468 Dorf, M., Bösch, H., Butz, A., Camy-Peyret, C., Chipperfield, M. P., Engel, A., Goutail, F.,
469 Grunow, K., Hendrick, F., Hrechanyy, S., Naujokat, B., Pommereau, J.-P.,
470 Van Roozendael, M., Sioris, C., Stroh, F., Weidner, F., and Pfeilsticker, K.: Balloon-borne
471 stratospheric BrO measurements: comparison with Envisat/SCIAMACHY BrO limb profiles,
472 Atmos. Chem. Phys., 6, 2483-2501, doi:10.5194/acp-6-2483-2006, 2006a.
473 Dorf, M., Butler, J. H., Butz, A., Camy-Peyret, C., Chipperfield, M. P., Kritten, L., Montzka, S.
474 A., Simmes, B., Weidner, F., and Pfeilsticke, K.: Long-term observations of stratospheric
475 bromine reveal slow down in growth, Geophys. Res, Lett., 33, L24803,
476 doi:10.1029/2006GL027714, 2006b.
477 Dorf, M., Butz, A., Camy-Peyret, C., Chipperfield, M. P., Kritten, L., and Pfeilsticker, K.:
478 Bromine in the tropical troposphere and stratosphere as derived from balloon-borne BrO
479 observations, Atmos. Chem. Phys., 8, 7265–7271, 2008.
480 Douglass, A. R. and Kawa, S. R.: Contrast between 1992 and 1997 high-latitude spring Halogen
481 Occultation Experiment observations of lower stratospheric HCl, J. Geophys. Res.,
482 104(D15), 18739–18754, doi:10.1029/1999JD900281, 1999.

Dvortsov, V. L., Geller, M. A., Solomon, S., Schauffler, S. M., Atlas, E. L., and Blake, D. R.: Rethinking reactive halogen budgets in the midlatitudes lower stratosphere, Geophys. Res. Lett., 26, 1699– 1702, 1999.

Fueglistaler, S., Wernli, J. and Peter, T.: Tropical troposphere-to-stratosphere transport inferred from trajectory calculations, J. Geophys. Res., 109, D03108, doi:10.1029/2003JD04069, 2004.

Fueglistaler, S., Dessler, A. E., Dunkerton, T. J., Folkins, I., Fu, Q., and Mote, P. W.: Tropical tropopause layer, Rev. Geophys., 47, 1, doi:10.1029/2008RG000267, 2009.

Gettelman, A., and Forster, P. M. D. F.: A climatology of the tropical tropopause layer, J. Meteorol. Soc. Jpn., 80, 911-924, 2002.

Ginoux, P., Chin, M., Tegen, I., Prospero, J., Holben, B., Dubovik, O., and Lin, S.-J.: Sources and distributions of dust aerosols simulated with the GOCART model, J. Geophys. Res., 106, 20 225–20 273, 2001.

Giorgi, F., and Chameides, W. L.: Rainout lifetimes of highly soluble aerosols and gases as inferred from simulations with a general circulation model, J. Geophys. Res., 91, 14,367-14,376, 1986.

Hatsushika, H., and Yamazaki, K.: Stratospheric drain over Indonesia and dehydration within the tropical tropopause layer diagnosed by air parcel trajectories, J. Geophys. Res., 108(D19), 4610, doi:10.1029/2002JD002986, 2003.

Hossaini, R., Chipperfield, M. P., Monge-Sanz, B. M., Richards, N. A. D., Atlas, E., and Blake, D. R.: Bromoform and dibromomethane in the tropics: a 3-D model study of chemistry and transport, Atmos. Chem. Phys., 10, 719-735, 2010.

Hossaini, R., Chipperfield, M. P., Feng, W., Breider, T. J., Atlas, E., Montzka, S. A., Miller, B. R., Moore, F., and Elkins, J.: The contribution of natural and anthropogenic very short-lived species to stratospheric bromine, Atmos. Chem. Phys., 12, 371-380, doi:10.5194/acp-12-371-2012, 2012a.

Hossaini, R., Chipperfield, M. P., Dhomse, S., Ordonez, C., Saiz-Lopez, A., Abraham, N. L., Archibald, A., Braesicke, P., Telford, P., Warwick, N., Yang, X. and Pyle, J.: Modelling future changes to the stratospheric source gas injection of biogenic bromocarbons." Geophysical Research Letters, 39, L20813, doi:10.1029/2012GL053401, 2012b.

Hossaini, R., Mantle, H., Chipperfield, M. P., Montzka, S. A., Hamer, P., Ziska, F., Quack, B., Krüger, K., Tegtmeier, S., Atlas, E., Sala, S., Engel, A., Bönisch, H., Keber, T., Oram, D., Mills, G., Ordóñez, C., Saiz-Lopez, A., Warwick, N., Liang, Q., Feng, W., Moore, F., Miller, B. R., Marécal, V., Richards, N. A. D., Dorf, M., and Pfeilsticker, K.: Evaluating global emission inventories of biogenic bromocarbons, Atmos. Chem. Phys. Discuss., 13, 12485-12539, doi:10.5194/acpd-13-12485-2013, 2013.

Hoyle, C. R., Marécal, V., Russo, M. R., Allen, G., Arteta, J., Chemel, C., Chipperfield, M. P., D'Amato, F., Dessens, O., Feng, W., Hamilton, J. F., Harris, N. R. P., Hosking, J. S., Lewis, A. C., Morgenstern, O., Peter, T., Pyle, J. A., Reddmann, T., Richards, N. A. D., Telford, P. J., Tian, W., Viciani, S., Volz-Thomas, A., Wild, O., Yang, X., and Zeng, G.: Representation of tropical deep convection in atmospheric models – Part 2: Tracer transport, Atmos. Chem. Phys., 11, 8103-8131, doi:10.5194/acp-11-8103-2011, 2011.

Kreycy, S., Camy-Peyret, C., Chipperfield, M. P., Dorf, M., Feng, W., Hossaini, R., Kritten, L., Werner, B., and Pfeilsticker, K.: Atmospheric test of the $J(BrONO_2)/k_{BrO+NO2}$ ratio: implications for total stratospheric Bry and bromine-mediated ozone loss, Atmos. Chem. Phys., 13, 6263-6274, doi:10.5194/acp-13-6263-2013, 2013.

529 Kurylo, M. J., and Rodriguez, J. M.: Short-lived ozone related compounds, in Scientific
530 Assessment of Ozone Depletion: 1998, Global Ozone Res. and Monit. Proj., Rep. 44, chap.
531 2, World Meteorol. Organ., Geneva, Switzerland. 1999.
532 Levine, J. G., Braesicke, P., Harris, N. R. P., Savage, N. H., and Pyle, J. A.: Pathways and
533 timescales for troposphere-to-stratosphere transport via the tropical tropopause layer and
534 their relevance for very short lived substances, J. Geophys. Res., 112,
535 doi:10.1029/2005JD006940, 2007.
536 Levine, J. G., Braesicke, P., Harris, N. R. P., Pyle, J. A.: Seasonal and inter-annual variations in
537 troposphere-to-stratosphere transport from the tropical tropopause layer, Atmos. Chem. Phys.
538 8, 3689-3703, 2008.
539 Liang, Q., Stolarski, R. S., Kawa, S. R., Nielsen, J. E., Douglass, A. R., Rodriguez, J. M.,
540 Blake, D. R., Atlas, E. L., and Ott, L. E.: Finding the missing stratospheric Bry: a global
541 modeling study of CHBr3 and CH2Br2, Atmos. Chem. Phys., 10, 2269-2286,
542 doi:10.5194/acp-10-2269-2010, 2010.
543 Lin, S.-J.: A "vertically Lagrangian" finite-volume dynamical core for global models, Mon.
544 Weather Rev., 132(10), 2293–2307, 2004.
545 Liu, H., Jacob, D. J., Bey, I., and Yantosca, R. M.: Constraints from 210Pb and 7Be on wet
546 deposition and transport in a global three-dimensional chemical tracer model driven by
547 assimilated meteorological fields, J. Geophys. Res., 106(D11), 12109–12128,
548 doi:10.1029/2000JD900839, 2001.
549 Moorthi, S., and Suarez, M. J.: Relaxed Arakawa–Schubert: A parameterization of moist
550 convection for general circulation models, Mon. Wea. Rev., 120, 978–1002, 1992.
551 Nielsen, J. E., and Douglass A. R.: A simulation of bromoform's contribution to stratospheric
552 bromine, J. Geophys. Res., 106, 8089– 8100, 2001.
553 Ordóñez, C., Lamarque, J.-F., Tilmes, S., Kinnison, D. E., Atlas, E. L., Blake, D. R.,
554 Sousa Santos, G., Brasseur, G., and Saiz-Lopez, A.: Bromine and iodine chemistry in a
555 global chemistry-climate model: description and evaluation of very short-lived oceanic
556 sources, Atmos. Chem. Phys., 12, 1423-1447, doi:10.5194/acp-12-1423-2012, 2012.
557 Ott, L. E., Bacmeister, J., Pawson, S., Pickering, K., Stenchikov, G., Suarez, M. Huntriester, H.,
558 Loewenstein, M., Lopez, J., and Xueref-Remy, I.: Analysis of Convective Transport and
559 Parameter Sensitivity in a Single Column Version of the Goddard Earth Observation System,
560 Version 5, General Circulation Model. *J. Atmos. Sci.*, **66**, 627–646, 2009.
561 Ott, L. E., Pawson, S., and Bacmeister, J.: An analysis of the impact of convective parameter
562 sensitivity on simulated global atmospheric CO distributions, J. Geophys. Res. 116, D21310,
563 doi:10.1029/2011JD016077, 2011.
564 Parrella, J. P., Jacob, D. J., Liang, Q., Zhang, Y., Mickley, L. J., Miller, B., Evans, M. J., Yang,
565 X., Pyle, J. A., Theys, N., and Van Roozendael, M., Atmos. Chem. Phys., 12, 6723-6720,
566 doi:10.5194/acp-12-6723-2012, 2012.
567 Pyle, J. A., Ashfold, M. J., Harris, N. R. P., Robinson, A. D., Warwick, N. J., Carver, G. D.,
568 Gostlow, B., O'Brien, L. M., Manning, A. J., Phang, S. M., Yong, S. E., Leong, K. P.,
569 Ung, E. H., and Ong, S.: Bromoform in the tropical boundary layer of the Maritime
570 Continent during OP3, Atmos. Chem. Phys., 11, 529-542, doi:10.5194/acp-11-529-2011,
571 2011.
572 Randel, W. J., and Jensen, E. J.: Physical processes in the tropical tropopause layer and their role
573 in a changing climate, Nature Geoscience, 6, 169-176, doi:10.1038/ngeo1733, 2013.

574 Reinecker, M. M, Suarez, M. J., Todling, R., Bacmeister, J., Takacs, L., Liu, H.-C., Gu, W.,
575 Sienkiewicz, M., Koster, R. D., Gelaro, R., Stajner, I., and Nielsen, J. E.: The GEOS-5 Data
576 Assimilation System-Documentation of Versions 5.0.1, 5.1.0, and 5.2.0, Tech. Rep. 104606
577 V27, NASA, Greenbelt, MD, 2008.
578 Rozanov, A., Kühl, S., Doicu, A., McLinden, C., Puķīte, J., Bovensmann, H., Burrows, J. P.,
579 Deutschmann, T., Dorf, M., Goutail, F., Grunow, K., Hendrick, F., von Hobe, M.,
580 Hrechanyy, S., Lichtenberg, G., Pfeilsticker, K., Pommereau, J. P., Van Roozendael, M.,
581 Stroh, F., and Wagner, T.: BrO vertical distributions from SCIAMACHY limb
582 measurements: comparison of algorithms and retrieval results, Atmos. Meas. Tech., 4, 1319-
583 1359, doi:10.5194/amt-4-1319-2011, 2011.
584 Sander, S. P., Abbatt, J. P. D., Barker, J. R., Burkholder, J. B., Golden, D. M., Kolb, C. E.,
585 Kurylo, M. J., Moortgat, G. K., Wine, P. H., Huie, R. E., Orkin, V. L.: Chemical Kinetics and
586 Photochemical Data for Use in Atmospheric Studies: Evaluation No. 17, JPL Publ. 10-6, Jet
587 Propul. Lab., Pasadena, CA, USA, 2011.
588 Salawitch, R. J., Canty, T., Kurosu, T., Chance, K., Liang, Q., da Silva, A., Pawson, S., Nielsen,
589 J. E., Rodriguez, J. M., Bhartia, P. K., Liu, X., Huey, L. G., Liao, J., Stickel, R. E., Tanner,
590 D. J., Dibb, J. E., Simpson, W. R., Donohoue, D., Weinheimer, A., Flocke, F., Knapp, D.,
591 Montzka, D., Neuman, J. A., Nowak, J. B., Ryerson, T. B., Oltmans, S., Blake, D. R., Atlas,
592 E. L., Kinnison, D. E., Tilmes, S., Pan, L. L., Hendrick, F., Van Roozendael, M., Kreher, K.,
593 Johnston, P. V., Gao, R. S., Johnson, B., Bui, T. P., Chen, G., Pierce, R. B., Crawford, J. H.,
594 and Jacob, D. J.: A new interpretation of total column BrO during Arctic spring, Geophys.
595 Res. Lett., 37, L21805, doi:10.1029/2010GL043798, 2010.
596 Schauffler, S. M., Atlas, E. L., Blake, D. R., Flocke, F., Lueb, R. A., Lee-Taylor, J. M., Stroud,
597 V., and Travnicek, W.: Distributions of brominated organic compounds in the troposphere
598 and lower stratosphere, J. Geophys. Res., 104 (D17), 21513-21535, 1999.
599 Sinnhuber, B.-M., Rozanov, A., Sheode, N., Afe, O. T., Richter, A., Sinnhuber, M., Wittrock, F.,
600 Burrows, J. P., Stiller, G.P., von Clarmann, T., and Linden ,A.: Global observations of
601 stratospheric bromine monoxide from SCIAMACHY, Geophys. Res. Lett., 32, L20810, doi:
602 10.1029/2005GL023839, 2005.
603 Sinnhuber, B.-M. and Folkins, I.: Estimating the contribution of bromoform to stratospheric
604 bromine and its relation to dehydration in the tropical tropopause layer, Atmos. Chem. Phys.,
605 6, 4755–4761, 2006.
606 Sioris, C.E., Kovalenko, L. J., McLinden, et al.:, Latitudinal and vertical distribution of bromine
607 monoxide in the lower stratosphere from Scanning Imaging Absorption Spectrometer for
608 Atmospheric Chartography limb scattering measurements, J. Geophys. Res., 111, D14301,
609 doi: 10.1029/2005JD006479, 2006.
610 Spivakovsky, C. M., Logan, J. A., Montzka, S. A., Balkanski, Y. J., M. Foreman-Fowler, ones,
611 D. B. A., Horowitz, L. W., Fusco, A. C., Brenninkmeijer, C. A. M., Prather, M. J., Wofsy, S.
612 C., and McElroy, M. B.: Three-dimensional climatological distribution of tropospheric OH:
613 Update and evaluation, J. Geophys. Res., 105, 8931–8980, 2000.
614 Sturges, W.T., Oram, D. E., Carpenter, L. J., Penkett, S. A. and Engel, A.: Bromoform as a
615 source of stratospheric bromine, Geophys. Res. Lett., 27 (14), 2081-2084, 2000.
616 Warwick, N. J., Pyle, J. A., Carver, G. D., Yang, X., Savage, N. H., O'Connor, F. M., and Cox,
617 R. A.: Global modeling of biogenic bromocarbons, J. Geophys. Res., 111, D24305,
618 doi:10.1029/2006JD007264, 2006.
619 Webster, P. J.: The large scale structure of the tropical atmosphere, General Circulation of the

Atmosphere, Academic Press, pp. 235-275, 1983.
WMO (2011), Scientific Assessment of Ozone Depletion: 2010, Global Ozone Research and Monitoring Project-Report No. 52, 516 pp., Geneva, Switzerland.
Yang, X., Cox, R. A., Warwick, N. J., Pyle, J. A., Carver, G. D., and O'Connor F. M.: Tropospheric bromine chemistry and its impacts on ozone: A model study, J.Geophys. Res., 110, D23311, doi: 10.1029/2005-JD006244, 2005.
Ziska, F., Quack, B., Abrahamsson, K., Archer, S. D., Atlas, E., Bell, T., Butler, J. H., Carpenter, L. J., Jones, C. E., Harris, N. R. P., Hepach, H., Heumann, K. G., Hughes, C., Kuss, J., Krüger, K., Liss, P., Moore, R. M., Orlikowska, A., Raimund, S., Reeves, C. E., Reifenhäuser, W., Robinson, A. D., Schall, C., Tanhua, T., Tegtmeier, S., Turner, S., Wang, L., Wallace, D., Williams, J., Yamamoto, H., Yvon-Lewis, S., and Yokouchi, Y.: Global sea-to-air flux climatology for bromoform, dibromomethane and methyl iodide, Atmos. Chem. Phys., 13, 8915-8934, doi:10.5194/acp-13-8915-2013, 2013.

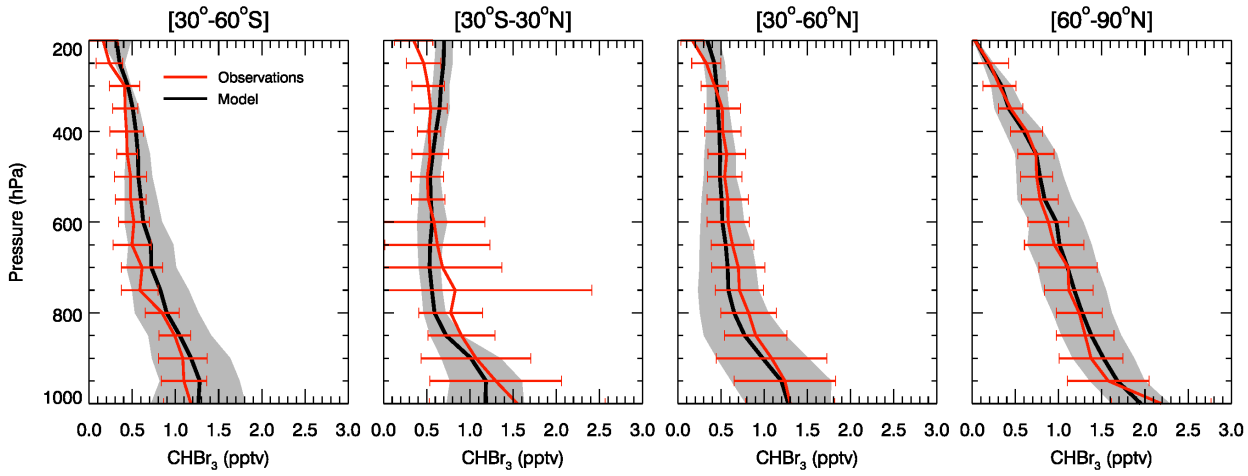

Figure 1. Comparison between the observed (red lines with horizontal bars indicating one standard deviation) and simulated (black lines with gray shading showing one sigma variability) vertical profiles of $CHBr_3$ in the troposphere. Observations are compiled using Whole Air Sampler canister measurements from eight NASA aircraft missions are averaged for 30-60ºS, 30ºS-30ºN, 30-60ºN, and 60-90ºN latitude bands at 1-km vertical interval. Model is sampled at the same location as the observations in the corresponding month in 2010.

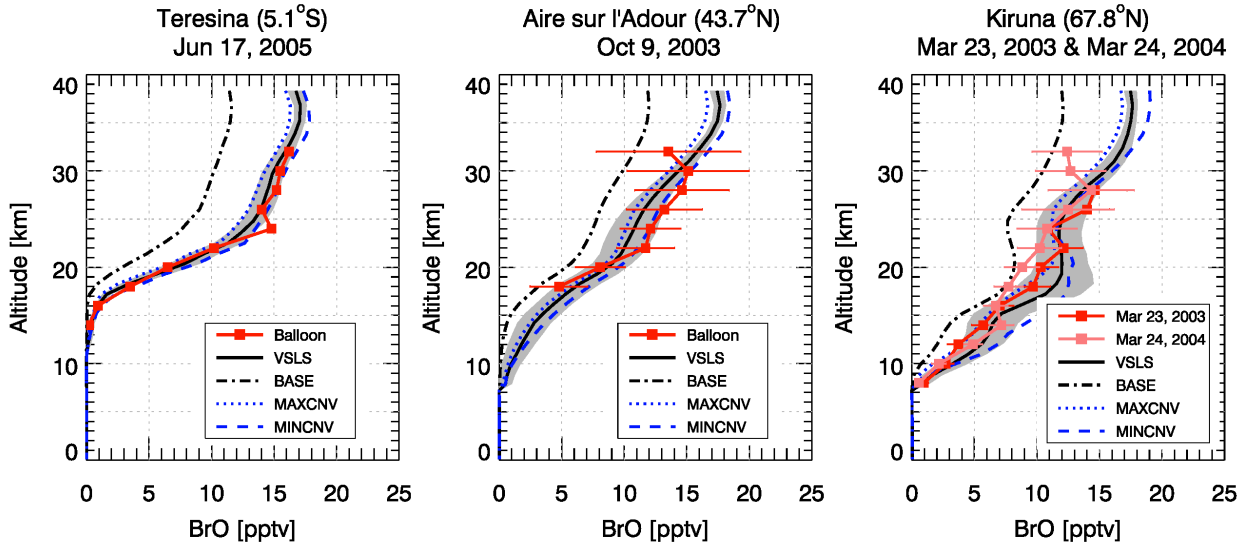

Figure 2. Comparison of simulated BrO from the GEOSCCM run R_{VSLS} (black solid line with 1-sigma variance in gray shading) with balloon measurements (red line with 1-sigma uncertainty in horizontal bars) from the LPMA/DOAS Spectrometers in the stratosphere. The black dash-dotted line shows simulated BrO from the run without VSLS (R_{BASE}). Simulated BrO from the two convective sensitivity simulations are also shown (dotted line for maximum convection condition and dashed line for minimum convection condition). The model is sampled at the same month and latitude as the balloon measurements but only daytime profiles from all available longitude grid points are collected to calculate the 1-sigma variance of simulated BrO.

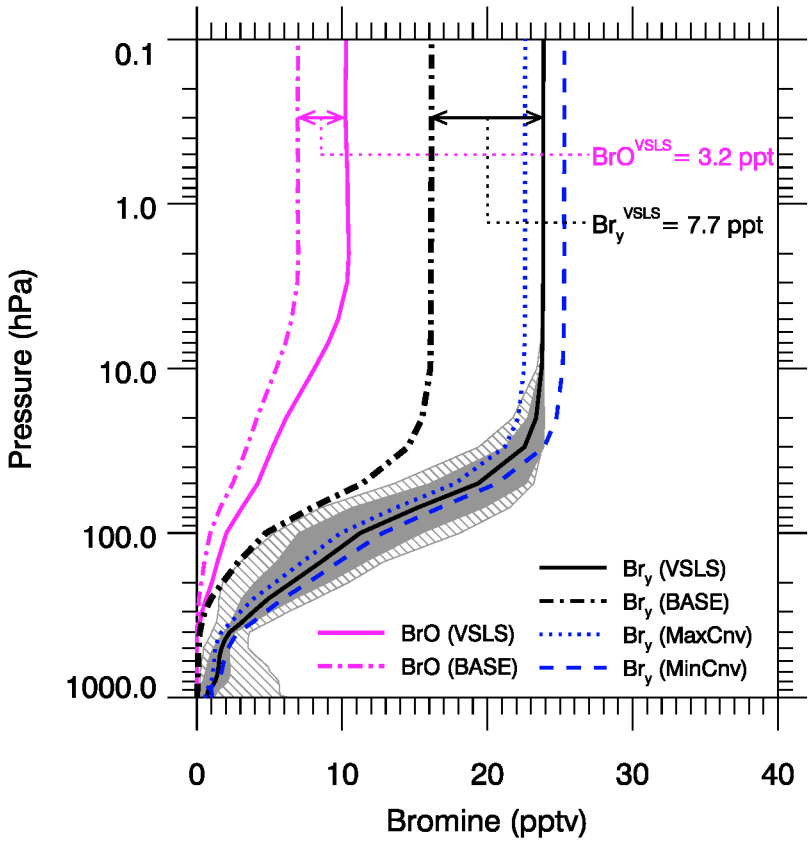

Figure 3. Model simulated global and annual mean BrO and Br_y profiles from the simulation with VSLS (R_{VSLS}, solid lines) and the base simulation without VSLS (R_{BASE}, dash-dotted lines) for Year 2010**.** The gray shadings indicate the spread of annual mean Br_y in the R_{VSLS} run with the hatched areas indicate the minimum to maximum range and the filled shadings indicate 1-sigma variance. Br_y from the two convective sensitivity simulations are also shown (blue dashed and dotted line for minimum and maximum convection conditions, respectively).

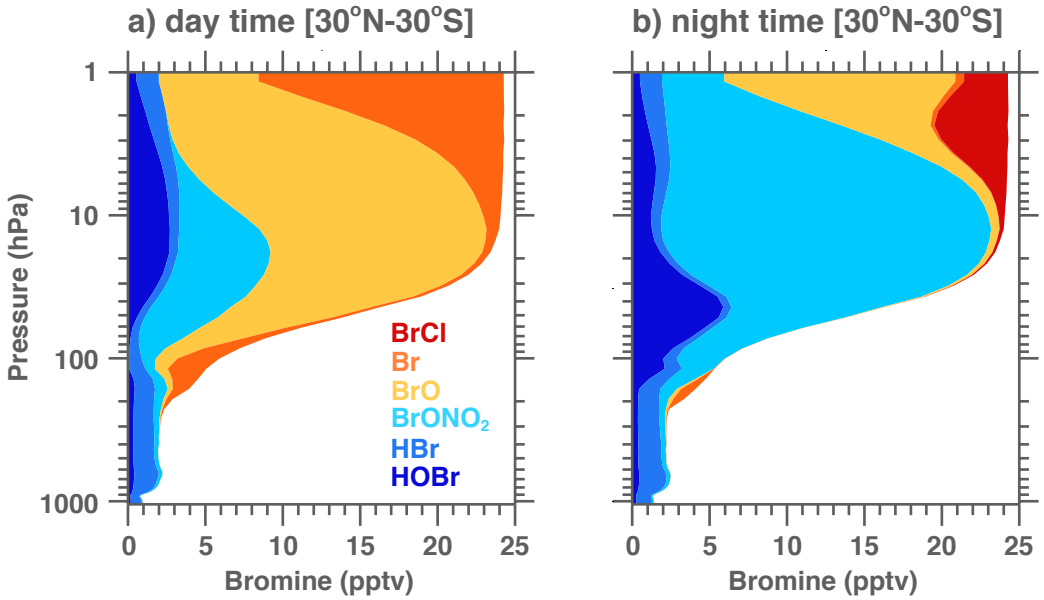

Figure 4. Annual mean model inorganic bromine (BrCl, Br, BrO, $BrONO_2$, HBr, HOBr) tropical vertical profiles for daytime (left panel) and nighttime (right panel), averaged between 30ºN-30ºS.

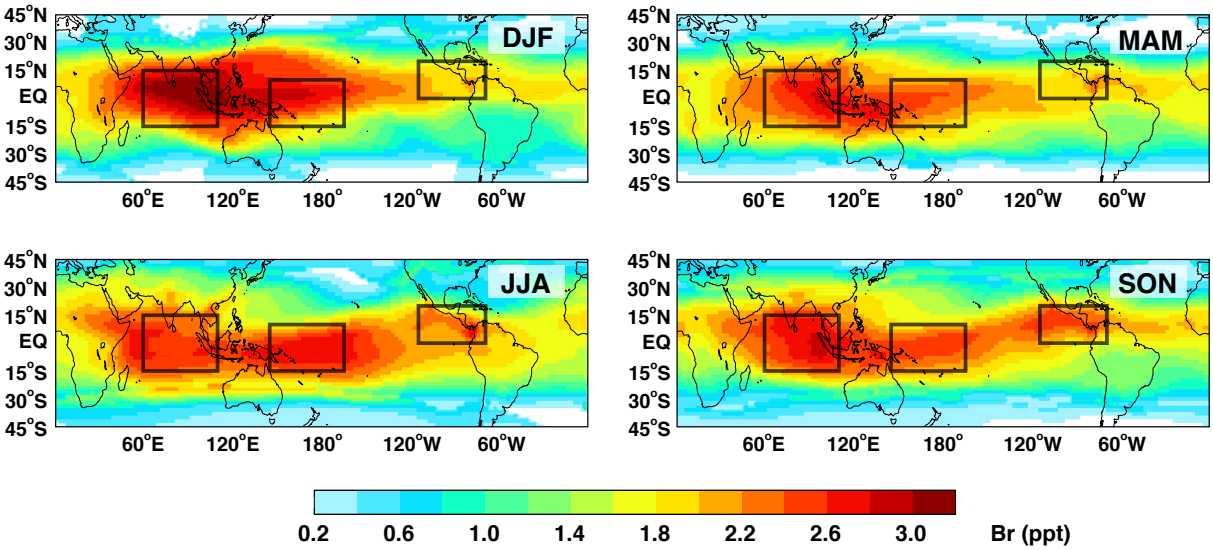

Figure 5. 10-year averaged (2001-2010) seasonal mean distribution of simulated $CHBr_3$ (unit ppt Br) at the 355K potential temperature layer (just below tropopause) in DJF, MAM, JJA and SON. The black boxes outline the three regions where most active troposphere-to-stratosphere transport occurs.

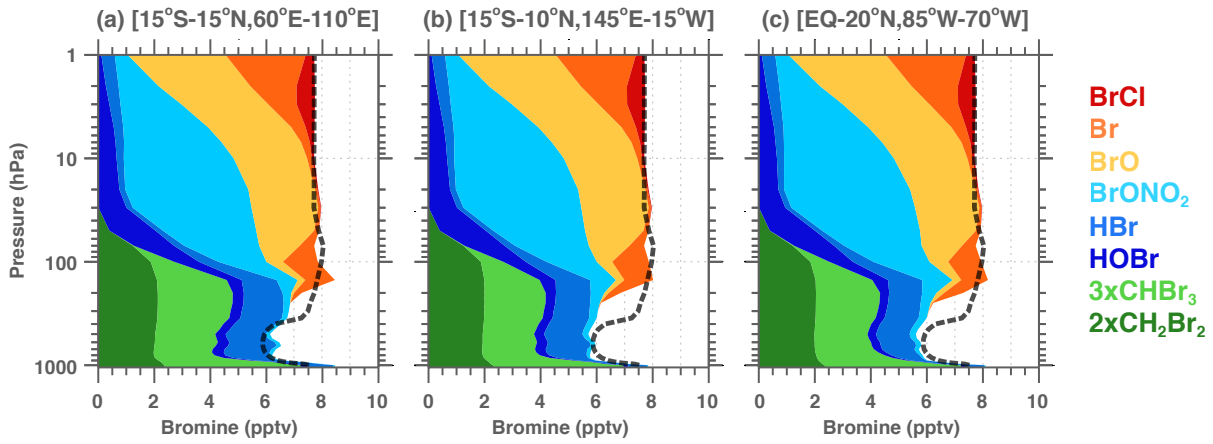

Figure 6. The contribution of organic bromine (CH_2Br_2×2, $CHBr_3$×3) and inorganic bromine (Br_y^{VSLS}) from $CHBr_3$ and CH_2Br_2 degradation to atmospheric bromine in three active TST regions (a) the tropical Indian Ocean (left), (b) the tropical western Pacific warm pool (middle), and (c) the Pacific Coast of Mexico (right). The soluble product gases (HBr, HOBr, $BrONO_2$) and insoluble product gases (Br, BrO, BrCl) are shown in blue colors and warm colors, repectively. The global mean sum of organic and inorganic bromine from VSLS is also shown (thick black dashed line). The model results are 10-year annual averages from 2001-2010.

686

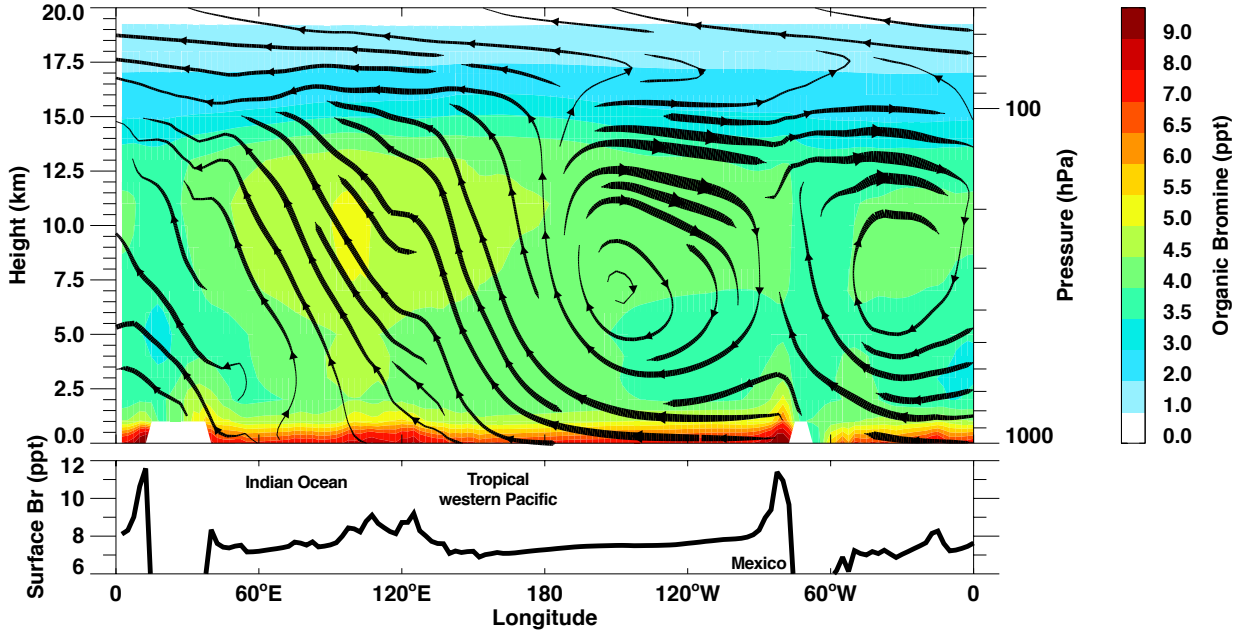

687
688 **Figure 7**. Longitude-height cross-section of modeled total VSL organic bromine ($CHBr_3 \times 3 +$
689 $CH_2Br_2 \times 2$) (color contours) and streamlines (black lines) in the deep tropics. The organic
690 bromine and wind streams are 10-year annual averages (2001-2010) between 10°S-10°N.
691 Surface organic bromine abundance is shown as the black solid line at the bottom panel.
692

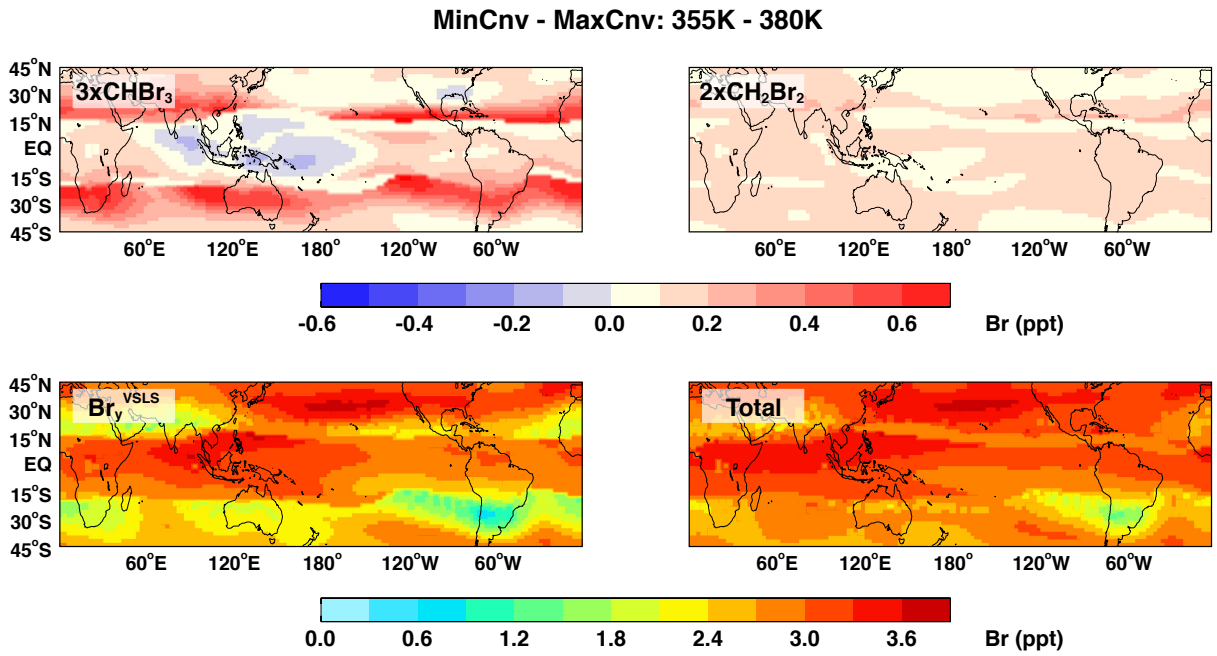

Figure 8. The simulated annual mean difference between the R_{MINCNV} and R_{MAXRUN} runs in organic bromine ($3\times CHBr_3$, $2\times CH_2Br_2$), inorganic bromine and total bromine from VSLS between 355-380K. The model results are 10-year annual averages from 2001-2010.